High Throughput MIMO-OFDM WLAN for Urban Hotspots

Y. Q. Bian, A. R. Nix, E. K. Tameh and J. P. McGeehan
Centre for Communications Research (CCR), University of Bristol,
Woodland Rd, Bristol, BS8 1UB, UK
{y.q.bian; andy.nix; tek.tameh; j.p.mcgeehan}@bristol.ac.uk

Abstract—**This paper presents a set of rigorous and comprehensive coverage and throughput studies for enhanced high-capacity Multi-Input Multi-Output Orthogonal Frequency Division Multiplexing (MIMO-OFDM) systems. A ray-tracing propagation model has been used to produce site-specific MIMO channel data. Site-specific throughputs are then predicted in a city centre environment for a range of different physical layer configurations. Dynamic Transmit Power Control (TPC) is applied to lower transmit power and thus reduce interference. Results demonstrate the need for suitable link adaptation strategies under a wide range of channel conditions. Spatial Multiplexing (SM) is shown to struggle in regions close to the basestation, or for locations with low SNR. We conclude that it is vital to reconfigure parameters on a case by case basis. When a suitable space-time algorithm is combined with Adaptive Modulation and Coding (AMC) and the appropriate number of antenna elements, high peak throughputs and good geographic coverage become realistic for wireless applications in a dense urban environment.**

Keywords-OFDM; MIMO; Space Time Block Codes; Spatial Multiplexing; Power Control; Link Adaptation

I. INTRODUCTION

An ever crowded radio spectrum implies that future demands must be met using more spectrally efficient wireless technologies. It is well reported in the literature that MIMO physical (PHY) layer techniques have the potential to significantly increase bandwidth efficiency in a rich scattering environment [1]. Coded Orthogonal Frequency Division Multiplexing (COFDM) is a well-established technique for achieving low-cost broadband wireless connectivity, and has been chosen as the air interface for a range of new standards, including IEEE802.11a/g and IEEE802.16d/e. The ideas of MIMO and OFDM have been combined by a number of authors to form a new class of MIMO-OFDM system [2][3]. This approach represents a promising candidate for hotspot (802.11) and urban last-mile (802.16) applications.

Radio propagation characteristics result in space selective fading and this can limit the level of spectral efficiency. The Foschini capacity equation [4] gives theoretic upper bound MIMO capacities. Accurate MIMO channel modelling is vital for practical system studies. The TGn802.11n channel models (Models A-F) were developed by the IEEE for evaluating multi-antenna element WLAN systems [5]. While these models can be used to evaluate a range of MIMO PHY layer candidates, the models require the Access Point (AP) and Mobile Station (MS) to be located in similar surrounding environments. This is not normally the case for outdoor urban applications. Many of the underlying assumptions make the parameter based TGn802.11n model questionable for link adaptation studies. Instead of using this model, we create a MIMO channel matrix for each AP-MS link using a site specific ray tracing model. Hence, the resulting spatial and temporal correlations match more closely those seen in practice [6]. For real application environments, very high Signal to Noise Ratios (SNR) are often observed by terminals near to the AP, and these are often far higher than that required by the mobile receiver. Maintaining a high SNR level at the cell edge requires a high transmit power, and this can cause high levels of interference to other users. Hence, Transmit Power Control (TPC) must be carefully considered. The peak capacity and QoS strongly depends on the PHY layer configuration, such as the choice of modulation and coding scheme, the selected space-time processing algorithm, and the detection technique. Higher order modulation schemes with Spatial Multiplexing (SM) increase the link throughput, but require high SNR to achieve low Packet Error Rates (PER). Space-Time Block Coding (STBC) provides strong diversity gain, but cannot increase the link throughput without the use of Adaptive Modulation and Coding (AMC). This paper presents a reconfigurable system that combines these requirements. Out analysis is based on a unique combination of urban ray tracing and site specific PHY layer MIMO modelling. We demonstrate the area-wide influence of received power and channel conditions for urban MIMO-OFDM applications. We compare the suitability of STBC and SM in a realistic urban environment. Link adaptation is introduced to determine the most appropriate PHY layer parameters. Results provide a valuable insight into the levels of coverage and capacity that can be achieved in more practical environments.

The paper is organized as follows: Section II introduces two methods for MIMO H-matrix generation. Section III describes the PHY layer modelling. Section IV presents simulation results with conclusions given in section V.

II. MIMO CHANNEL MODELLING

The MIMO channel capacity is commonly defined by the Foschini capacity equation [4]. When applying OFDM, the data stream is multiplexed into N_f narrowband subcarriers. If the channel is unknown, the channel capacity for a MIMO-OFDM system can be mathematically written as [1]

$$C \approx \frac{1}{N_f}\sum_{j=1}^{N_f}\log_2 \det\left(I_{N_R} + \frac{\rho}{N_T}\mathbf{H}_j\mathbf{H}_j^H\right) \quad b/\mathrm{sec}/Hz \qquad (1)$$

where ρ, N_T and N_R are the SNR, the number of transmitters and the number of receivers respectively. $\mathbf{H}_j$ (N_R –by- N_T) represents the frequency response of the MIMO H-matrix for the j-th subcarrier and $(.)^H$ denotes the Hermitian function. Equation (1) indicates that the MIMO capacity is directly affected by the SNR and the quality of the MIMO channel. MIMO channels can suffer from high spatial correlation, especially when the K-factor is high, the element spacings are low, or the Angular Spread (AS) is low.

This work has been funded by the Toshiba Telecommunications Research Laboratory (TRL), Bristol, UK.

A. *Parameter based model*

In this model, the MIMO H-matrix for a given tap in the channel impulse response (CIR) is separated into a fixed LoS matrix ($\mathbf{H}_{LoS}$) and a Rayleigh NLoS matrix ($\mathbf{H}_{Rayleigh}$) [1][7].

$$\begin{aligned}\mathbf{H}_l &= \sqrt{P_l}\left(\sqrt{\frac{K}{1+K}}\mathbf{H}_{LoS} + \sqrt{\frac{1}{1+K}}\mathbf{H}_{Rayleigh}\right)\\ &= \sqrt{P_l}\left(\sqrt{\frac{K}{1+K}}\begin{bmatrix} e^{j(\varphi+\Delta\phi_{1,1})} & \cdots & e^{j(\varphi+\Delta\phi_{1,N_T})} \\ \vdots & \ddots & \vdots \\ e^{j(\varphi+\Delta\phi_{N_R,1})} & \cdots & e^{j(\varphi+\Delta\phi_{N_R,N_T})}\end{bmatrix}\right.\\ &\quad\left. + \sqrt{\frac{1}{1+K}}\begin{bmatrix} X_{1,1} & \cdots & X_{1,N_T} \\ \vdots & \ddots & \vdots \\ X_{N_R,1} & \cdots & X_{N_R,N_T}\end{bmatrix}\right)\end{aligned} \quad (2)$$

where K and P_l, represent the Ricean K-factor and the power of the l-th tap; and $e^{j(\varphi+\Delta\phi_{n,m})}$ and $X_{n,m}$ are elements of $\mathbf{H}_{LoS}$ and $\mathbf{H}_{Rayleigh}$ for the n-th receiving and m-th transmitting antenna. For the LoS ray, φ and $\Delta\phi_{n,m}$ denote the initial reference phase and the phase difference that results when the m-th transmit antenna is used with the n-th receive antenna. $\mathbf{H}_{Rayleigh}$ is obtained by utilizing receive and transmit correlation matrices ($\mathbf{R}_{rx}$ and $\mathbf{R}_{tx}$).

$$\mathbf{H}_{rayleigh} = \mathbf{R}_{rx}^{1/2}\mathbf{H}_{iid}\mathbf{R}_{tx}^{1/2} \quad (3)$$

where $\mathbf{H}_{iid}$ is an independent and identically distributed (spatially white) MIMO channel. To calculate the correlation coefficients in $\mathbf{R}_{rx}$ and $\mathbf{R}_{tx}$, the AS and the Power Angle Spectrum (PAS) must be known [1]. With the TGn802.11n model, the K-factor is only modelled for the first tap and all remaining taps in the cluster follow a Rayleigh distribution. The Root Mean Square (RMS) AS is calculated based on the RMS Delay Spread (DS). The mean angle of arrival and departure are assigned to each cluster based on uniform random variables in the range [0~2π]. Identical distributions are assumed at both the transmitter and receiver, however, this is not observed in our ray model (since the MS is often in a different environment type relative to the AP). Moreover, there is no simple relationship between the RMS DS and the RMS AS for a typical urban environment, as shown in Fig. 1. When models E (RMS DS = 100 ns) and F (RMS DS = 150ns) are used for outdoor hot-spots, large AS values result in an over prediction of capacity.

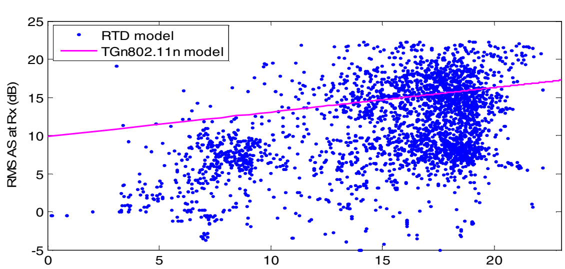

Figure 1. AS versus DS at receiver

B. *Ray Tracing Deterministic (RTD) model*

The use of ray-tracing provides accurate estimates for the Channel Impulse Response (CIR) and the PAS at both ends of the link, without the need for specific assumptions. The tool used in this paper traces electromagnetic waves in 3-D space and takes into account individual buildings, trees, corner and roof-top edges, terrain blocking and scattering. The ray model has been previously validated using measurement data collected in mixed urban and rural environments at 1.8 GHz and 5.2 GHz [6][8].

For the RTD MIMO channel model, MIMO H-matrices are fully determined from the predicted multipath components between the AP and each MS. Based on ray power (P_q), phase (φ_q), delay, and angle of arrival/departure for the q-th multipath component, it is possible to derive the channel coefficients of the q-th ray for the [n,m]-th link. This can be written as

$$H_{n,m}^{q}(t) = \sqrt{P_q}\, e^{j(\varphi_q + \Delta\phi_{n,m}^{q} + \Delta\theta_q)} \quad (4)$$

where $\Delta\varphi_{n,m}^{q}$ is a phase shift for the [n,m]-th link and $\Delta\theta_q$ is a random (uniform) and independently distributed phase shift. This later angle is used to create independent fading samples (except for the LoS ray). The H-matrices are determined using the following procedure:

1. Perform Ray Tracing from the AP to the MS,
2. Apply random phase to all the NLoS multipaths,
3. Generate the H-matrix for each ray based on the [m,n] array geometries,
4. Apply time binning to the [m,n]-th H-matrix (based on the bandwidth) to generate the CIR for the [m,n]-th link,
5. Fourier transform each CIR to generate the [m,n]-th frequency response at each OFDM sub-carrier.

Steps 2-5 are repeated as necessary to achieve a statistically large set of channels for PHY layer PER averaging. Hence, spatial correlations are determined by the antenna geometries and the multipath angular spreads. Frequency domain correlations between OFDM sub-bands are determined by the time delay spread. The disparity between the TGn802.11n model and the ray traced data is at its greatest in high K-factor channels. From the RTD model, the resulting spatial and temporal correlations match more closely those seen in practice. Finally, the use of predicted ray data allows the modelling of arbitrary antenna element geometries, patterns and polarizations at both the AP and MS.

Figure 2 illustrates an example for an instantaneous channel. It shows that each MIMO link has its own individual frequency power profile at each instant in time. All the MIMO links have identical mean power.

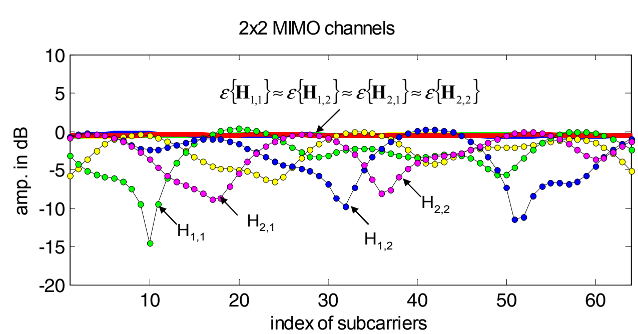

Figure 2. MIMO channel from RTD model

III. PHY LAYER MODELLING

MIMO-OFDM systems offer the potential for high spectral efficiency, substantial diversity gain and a strong immunity to inter-symbol interference. The received signal at each subcarrier can be expressed in matrix form as:

$$\mathbf{y}_j = \mathbf{H}_j \mathbf{x}_j + \mathbf{N}_j \tag{5}$$

where $\mathbf{x}_j$ (N_T -by-1 vector) and $\mathbf{N}_j$ (N_R -by-1 vector) denote the transmitted signal and the noise term at the j-th subcarrier.

A. Space-Time Coding (STC)

When T time slots are used to transmit k symbols, the rate of the STC is $R_{STC} = k/T$. A STC scheme can be defined by an N_T -by- T transmission matrix (**G**). Table I illustrates the four STC methods considered in this paper. A traditional Alamouti STBC scheme [9] uses two antennas to transmit two signals simultaneously and offers a similar level of diversity to maximal ratio combining. A 4x4 STBC was proposed in [10]. Since symbols are transmitted over the four antennas, this scheme offers more diversity gain than the traditional 2x2 STBC. For the hybrid structure [11], two Alamouti codes are used in parallel; this offers the same diversity gain as the 2x2 STBC case, but also increases capacity due to the additional SM. However, both the hybrid and the 4x4 STBC methods have partial orthogonality between each pair of transmit antennas. Detection techniques at the receiver for each scheme were described in [9][10][11]. Simple MMSE decoding [12] is applied for the SM and hybrid schemes, since here we focus on illustrating the general trends between SM, STBC and hybrid schemes.

TABLE I
STC METHOAD FOR MIMO TRANSMISSION

STC method	N_t	$\mathbf{G}^T$	R_{STC}
STBC	2	$\begin{bmatrix} x_1 & x_2 \\ -x_2^* & x_1^* \end{bmatrix}$	1
STBC	4	$\begin{bmatrix} x_1 & x_2 & x_3 & x_4 \\ x_2^* & -x_1^* & x_4^* & -x_3^* \\ x_3 & -x_4 & -x_1 & x_2 \\ x_4^* & x_3^* & -x_2^* & -x_1^* \end{bmatrix}$	1
hybrid	4	$\begin{bmatrix} x_1 & x_2 & x_3 & x_4 \\ -x_2^* & x_1^* & -x_4^* & x_3^* \end{bmatrix}$	2
SM	4	$\begin{bmatrix} x_1 & x_2 & x_3 & x_4 \end{bmatrix}$	4

B. Link adaptation

The IEEE 802.11 standard defines a range of modulation and coding schemes at the PHY layer [9]. Based on these, different MIMO system configurations can be applied (with different STC and AMC schemes) to achieve a given link throughput, as shown in figure 3. The peak throughput at the PHY layer is given by: $Throughput = D \times (1 - PER)$, where the transmission date rate is defined as: $D = \dfrac{N_D N_b R_{FEC} R_{STC}}{T_s}$, and N_D, N_b, R_{FEC} and T_s denote the number of data subcarriers, the coded bits per subcarriers, the coding rate and the OFDM symbol duration respectively. Table II lists the maximum throughput for a range of 4x4 MIMO-OFDM systems utilizing SM, STBC and the hybrid scheme with BPSK, QPSK and 16QAM. They all have a coding rate of ¾ and the results were generated for MS location rx #59 (see Fig. 4(a)), which has no dominant ray. Results show that to achieve the same level of peak throughput, the SM schemes need a high SNR compared to the STBC and hybrid schemes. For example, the required SNR for the STBC, hybrid and SM schemes are 5dB, 10dB and 25dB for a 36Mb/s throughput respectively. SM with 16QAM requires an even higher SNR value (60dB). It indicates that higher modulation schemes using SM need more transmit power to operate at low PER. STBC schemes offer diversity gains, but these come at the expense of a lower peak capacity. For link adaptation, a mode with the highest throughput and the lowest PER should be selected for each receive location. The link adaptation needs to combine STC with AMC. If more than one mode can provide a satisfactory PER for a specific transmit data rate, then the lowest modulation order should be chosen, since higher modulation schemes are more sensitive to phase jitter.

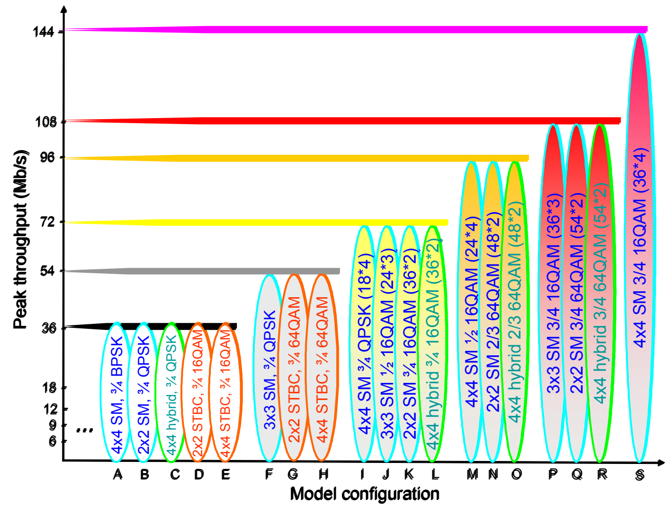

Figure 3. Peak throughput of different system configuration in 20MHz bandwidth

TABLE II
REQUIRED SNR FOR 4X4 MIMO-OFDM TO ACHIEVE PEAK THROUGHPUT

Models	STC method	Modulation	Peak throughput	Required SNR
Model A	SM	BPSK	36 Mb/s	25 dB
Model C	Hybrid	QPSK	36 Mb/s	10 dB
Model E	STBC	16QAM	36 Mb/s	5 dB
Model I	SM	QPSK	72 Mb/s	45 dB
Model L	Hybrid	16QAM	72 Mb/s	20 dB
Model S	SM	16QAM	144 Mb/s	60 dB

Channel conditions (rx #59): RMS AS at AP = 94.4 degrees; RMS AS at MS = 34.38 degrees; RMS DS = 65.05 ns

C. Tranmitter Power Control

In real wireless communication environments, path loss and shadowing cause low SNR at the receiver. [13] explored the normalization of $\mathbf{HH}^H$ and assumed perfect TPC. For practical networks, it is not possible to increase the transmit power level beyond a maximum regulated limit. When wireless systems employ link adaptation, the strategy of TPC needs to be carefully considered. If we consider a nominal power level (P_{nom}); dynamic TPC based on the received SNR (ρ) can be employed with three defined operating regions 1) in the high SNR region the transmit power (P_{tx}) is reduced in steps until the upper SNR threshold ($\rho_{\max}$) is reached; 2) in the low SNR region, P_{tx} is increased in steps until the received SNR reaches the minimum threshold ($\rho_{\min}$), or until P_{tx} reaches its maximum value $P_{tx,\max}$; 3) when $P_{tx}\big|_{\rho_{\min} < \rho \le \rho_{\max}} = P_{nom}$, no TPC is required. The value of ρ_{max} should be set based on the highest required SNR (which will normally depend on the highest throughput mode). Clearly, the value of P_{nom} will have a significant impact on the operating range of the highest throughput modes. For many deployments, this approach is desirable since there is the lowest level of throughput but the highest level of interference at the cell edge. For SM based PHY layers, where high SNR values are required, the use of a high P_{nom} level is recommended. For STBC based PHY layers, a lower value of P_{nom} may be beneficial in cellular (multi-AP) deployments. In this paper, STBC is used at the cell edge to achieve diversity gain; otherwise link adaptation is performed.

IV. Simulation Results

In this section, a complete set of simulation results (in terms of link capacity and area coverage) are presented. All parameters for the PHY layer simulations are assumed to follow the IEEE 802.11a standard [14], unless explicitly stated. A 40 MHz channel is assumed in order to achieve a 108 Mb/s throughput. The system noise temperature was 290 degrees Kelvin and a noise figure of 3 dB was assumed. Across a 400m x 400m region of central Bristol, MS were uniformly deployed at 5 meter spacings and a single AP was deployed at a height of 5 meters above ground level. Omni-directional antennas were arranged in the form of a ULA ($\lambda/2$ separations) at both the AP and MS. Dynamic TPC was applied with $\rho_{\max}$ = 30 dB, $\rho_{\min}$ = 15 dB, P_{nom} = 30 dB$_m$ and $P_{tx,\ \max}$ = 40 dB$_m$. MIMO fading channels were created using the output from the RTD model described previously, and static fading was assumed for every packet, which has a length of 1152 bytes. To evaluate area coverage, we define a maximum PER of 10%.

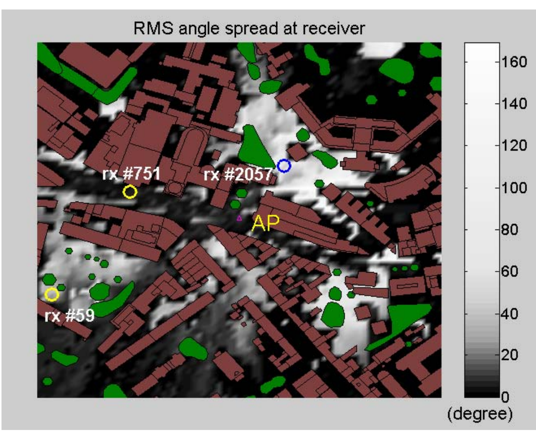

(a)

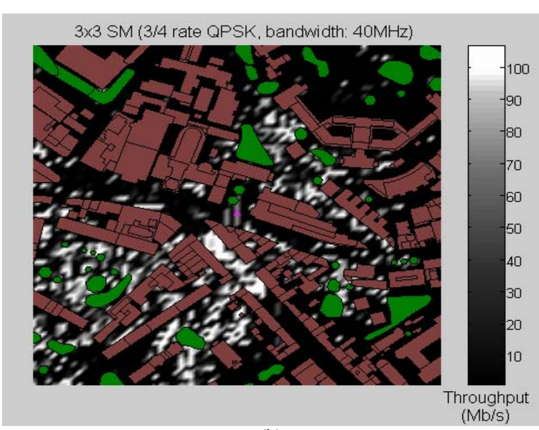

(b)

Figure 4. Grid Coverage Plots.

Fig. 4(a) presents the distribution of the RMS AS. Low correlated MIMO channels tend to have large RMS AS. Small values of RMS AS tend to occur in locations with strong LoS. In these cases a high degree of spatial correlation can occur, and this can have a detrimental effect on MIMO system performance, as shown in Fig. 4(b). Given that the SM schemes under test have a low immunity to high correlation values, this particular SM scheme cannot provide service for locations with low RMS AS or low SNR. When the MS moves close to the AP, due to the low RMS AS, and thus low H-matrix rank, the 3x3 SM scheme is unable to meet the 10% PER target even though the SNR is high.

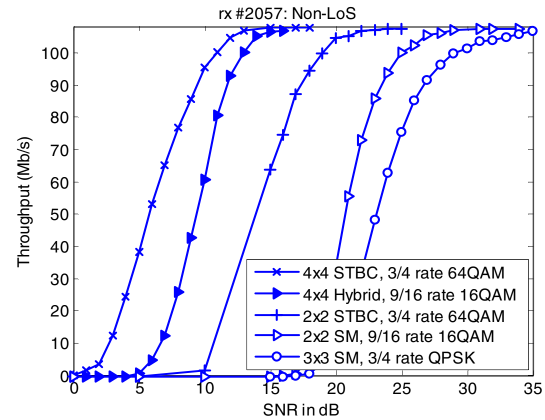

Figure 5. Non- LoS Analysis for rx: #2057. (K-factor = -3.3 dB; RMS AS at AP = 27.5 degrees; RMS AS at MS = 150.4 degrees; RMS DS = 66.8 ns)

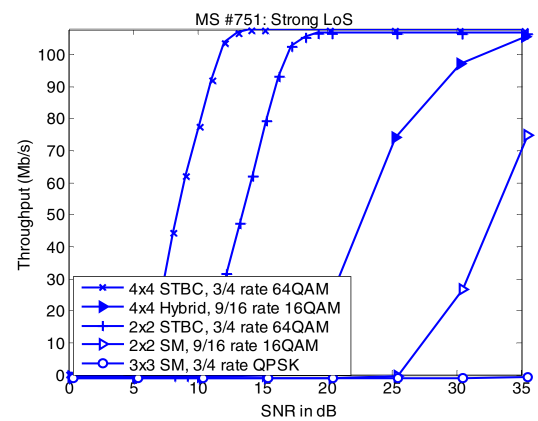

Figure 6. LoS Analysis for rx #751. (K-factor = 10dB; RMS AS at AP=11.8 degree; RMS AS at MS = 4 degrees; RMS DS = 5.6ns)

Figs. 5 and 6 present throughputs for the two particular test cases shown in Fig. 4(a); namely non-LoS (e.g., rx #2057) and LoS (e.g. rx #751). The same peak throughput of 108 Mb/s in a 40 MHz channel was assumed for all five simulated models. The use of identical peak throughputs enables a fair comparison to be drawn. If the channel is Non-LoS, the throughput for the 4x4 hybrid scheme using 16QAM is higher than the 2x2 STBC scheme using 64QAM over a wide range of SNR values (5-25 dB as shown in Fig. 5). The required SNR to achieve the peak throughput is 15 dB and 25 dB for the 4x4 hybrid and 2x2 STBC schemes respectively. However, if the channel has a LoS component, the throughput for the 4x4 hybrid scheme becomes much lower than that of the 2x2 STBC scheme. The required SNR to achieve the peak throughput also increases to 35 dB for the hybrid scheme, as shown in Fig. 6. Results indicate that 4x4 STBC offers a powerful diversity gain for both rx #2057 and rx #751.

In practice, high throughput at low SNR (and low receive complexity) is necessary. At each point in our hotspot, we choose the MIMO scheme from the above five models that maximizes the throughput. Fig.7 demonstrates that 87.7% of locations could be covered when using link adaptation. The SM system (Fig. 4(b)) only covers 23% of locations. Fig. 7 also indicates that the SM and hybrid schemes cannot operate close to the AP. SM is strongly preferred for most NLoS locations, other than those towards the cell edge. The hybrid scheme is used to capture diversity gain and extends coverage compared to standard SM. STBC is clearly preferred in LoS locations and for distant locations near the cell edge. Fig. 8 presents the link adaptation for a selected route in Fig. 7. Link adaptation strategies should be based on the channel conditions and SNR experienced at each point. For SM, low AS channels (e.g., rx #3) need higher SNR than larger AS channels (e.g., rx #18), and the minimum required SNR and RMS AS is 21 dB and 15 degrees, as shown in Fig. 8.

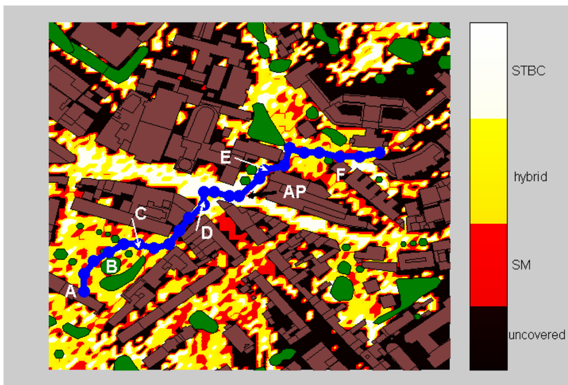

Figure 7. Area coverage for link adaptation

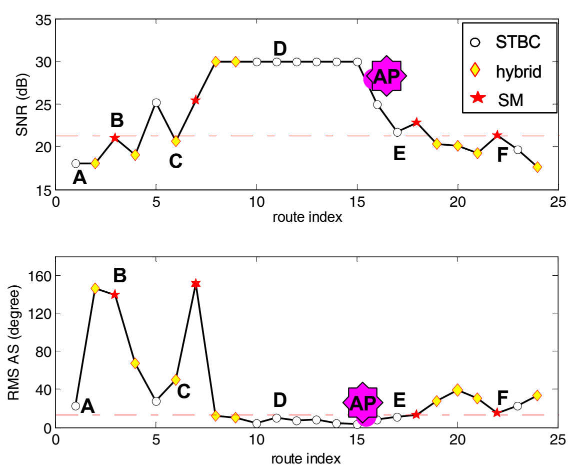

Figure 8. Link adaptation versus SNR and AS

V. CONCLUSIONS

Spatially correlated MIMO channels and the selected MIMO-OFDM system configuration at the PHY layer determine the level of spectral efficiency and QoS. Accurate MIMO channel modelling is vital for link adaptation studies. This paper has produced a unique view of the expected performance using a site specific RTD channel model and PHY simulations for an urban hotspot. The TGn802.11n channel models make many assumptions, some of which are not true for outdoor environments. The RTD MIMO channel model presents spatial and temporal correlations that match more closely those seen in practice. In order to i) increase coverage and throughput at low PER, ii) reduce transmit power, and iii) lower interference, link adaptation and dynamic TPC are recommended. Link adaptation combines AMC (based on IEEE 802.11a) with STC optimization (in our case choosing between STBC, SM and the hybrid scheme).

A key focus of this paper was the comparison of various STC methods under a wide range of channel conditions (both SNR and rank). Firstly, SM combined with higher order modulation was seen to increase the peak link throughput if full rank channels and high SNR is available. STBC offers diversity gain, but this comes at the expense of a lower peak capacity. For example, model S (4x4 SM, ¾ rate 16QAM) was shown to provide a peak throughput of 144 Mb/s, but requires an SNR greater than 60 dB, model E (4x4 STBC, ¾ rate 16QAM) was seen to offer strong diversity gains at low SNR (5 dB), but this method only achieves a peak throughput of 36 Mb/s. When STBC was combined with AMC (where high modulation schemes and coding rates are then selected), high peak throughputs can be reached. A reconfigurable system is attractive to combine these requirements. Link adaptation should be used to select the specific form of STC processing and AMC (and possibly antenna number and elements). This needs to take into account a wide range of channel conditions (both SNR and rank). This paper has shown that STBC is more suitable when the mobile is located in LoS to the AP (where the channel rank is low), or placed towards the cell edge (where the SNR is low). SM works well in locations with high SNR and rich multipath (indicated by wide RMS AS). For non-LoS regions, the hybrid STBC/SM scheme was seen to greatly enhance area coverage compared to standard SM, while also improving on the PER vs SNR performance of standard STBC. Any one MIMO scheme was unable to operate effectively over the entire service area. For our test environment, high capacity and good geographic coverage (87.7% of the service area) was achieved by selecting the most appropriate link technology.

REFERENCES

[1] A. Paulraj R. Nabar and D. Gore, *Introduction to space-time wireless communications*. Cambridge university press, 2003.

[2] H. Sampath, S. TAlwar, J. Tellado, V. Erceg and A. Paulraj, "A forth-generation MIMO-OFDM broadband wireless system: design performance, and field trial results," *IEEE Communications Magazine*, Vol. 40, No. 9, pp 143-149, Sep. 2002.

[3] A. Zelst and T. Schenk, "Implementation of a MIMO OFDM-based wireless LAN system," *IEEE Trans. Axoustics, Speech and Signal Processing,* Vol. 52, No. 2, pp 483-494, Feb. 2004.

[4] G. Foschini, "Layered space-time architecture for wireless communication in a fading environment when using multi-element antennas," *Bell Labs Tech.* J., 41-59, 1996.

[5] IEEE 802.11 wireless LANs, TGn channel models, doc. IEEE 802.11-03/940r4, May 2004.

[6] K, Ng, E. Tameh and A. Nix, "A new hybrid geometrical optics and radiance based scattering model for deterministic ray tracing model," IEEE ICC, May 2005.

[7] P. Soma, D. S. Baum, V. Erceg, R. Krishnamoorthy and A. J. Paulraj, "Analysis and modelling of multiple-output (MIMO) radio channel based on outdoor measurements conducted at 2.5 GHz for fixed BWA applications," in Proc. IEEE ICC Conf., April 2002.

[8] E. Tameh and A. Nix, "A mixed-cell propagation model for interference prediction in a UMTS network," IEEE VTC2001-spring, Vol.1, pp.409-

[9] M. Alamouti, "A simple transmit diversity technique for wireless communications," IEEE JSAC, Vol. 16, No. 8, Oct. 1998.

[10] C. Papadias and G. Foschini, "A space-time coding approach for systems employing four transmit antennas," IEEE ICASSP'01, Vol. 4, pp. 2481-2484, May 2001.

[11] A. Naguib, N. Seshadri and A. Calderbank, "Applications of space-time block codes and interference suppression for high capacity and high data rate wireless systems," Signals, Systems & Computers, Conference record of the Thirty-Second Asilomar Conference on, Vol. 2, pp. 1803-1810, Nov. 1998.

[12] M. Debbah, B. Muquet, M. Courville, M. Muck, S. Simoens and P. Loubaton, "A MMSE successive interference cancellation scheme for a new adjustable hybrid OFDM system," IEEE VTC-spring 2000. Vol. 2. pp. 745-749, May 2000.

[13] L. Dong, H. Ling and R. Heath Jr., "Multiple-input multiple-output wireless communication systems using antenna pattern diversity," IEEE GlOBECOM'02, Vol.1, pp.997-10001, Nov.2002.

[14] IEEE P802.11a/D7.0, "Draft supplement to standard for LAN/MAN part 11: MAC & PHY specifications," July 1999.